

Structural factors of amphiphilic calix[6]biscrowns affecting their vesicle–nanotube transitions in self-assembly†

Qing Liang, Guosong Chen, Bing Guan* and Ming Jiang*

Received 1st March 2011, Accepted 16th June 2011

DOI: 10.1039/c1jm10895f

Morphological transitions of self-assemblies of organic amphiphiles responsive to environmental stimuli have drawn much attention. However, little has been investigated regarding the effects of structural factors of calixarenes on their self-assembly behavior. In this paper, we studied the self-assembly of several amphiphilic calix[6]biscrowns with emphasis on morphological transitions of the assemblies with changes in medium polarity and the key structural factors of the calix[6]biscrowns affecting the transition. It was found that when the medium polarity increased, the calix[6]biscrowns with amide linkages between the backbone and the alkyl tails performed vesicle–nanotube transitions, while the calix[6]biscrowns without such linkages showed a decrease in size of the vesicles only. Further studies, including X-ray crystallography, FT-IR and Langmuir–Blodgett film, indicated that the hydrogen bonding between the amide linkages is responsible for this vesicle-to-nanotube transition. The effect of the nature of the end groups of the tails has also been studied.

1. Introduction

Self-assembly is a prevailing phenomenon in nature and is highlighted as a powerful practical strategy for fabricating nanostructures *via* proper designs of the building blocks.¹ Various assembled structures have been achieved, such as micelles,² vesicles,² nanotubes³ and ribbons,⁴ based on many different building blocks, including synthetic amphiphiles, block copolymers,⁶ dendrimers⁷ and biomacromolecules.⁵ Recently, great efforts have been devoted to manipulate transitions between different morphologies⁸ responsive to environmental changes, as it will endow the assemblies with possible tailored applications.

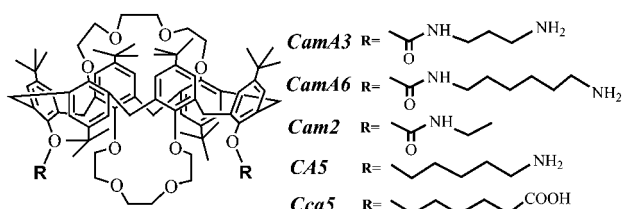
As a unique kind of building block for self-assembly, calixarenes have attracted specific attention during the past two decades,^{9–11} not only because of their well-known molecular cavities as hosts in supramolecular chemistry,¹² but also due to their relatively flexible and tunable molecular conformations, which provide versatile platforms to construct the desired well-defined nanomaterials.^{13–16} For instance, Lee's group¹⁷ reported that increasing the hydrophilic chain length of amphiphilic calix[4]arenes significantly decreased the diameter of the aggregates in

aqueous solution, from large vesicles to small spherical micelles, as a result of the increase in molecular curvature. Moreover, with a highly branched hydrophilic part introduced to the upper rim and the relatively smaller hydrophobic part modified on the lower rim, amphiphilic calixarenes self-assembled into precise and stable micelles.¹⁸ However, because of the rather flexible molecular backbone of the calixarenes, assemblies with regular shape or narrow size distributions were obtained¹⁹ only for those with bulky head groups, which greatly restricted the conformation change of the molecules. Very recently, unlike the popular spherical structures obtained by calixarene, a nanotubular structure fabricated from amphiphilic calix[4]resorcinarene was also reported, in which the co-contribution of intermolecular hydrogen bonds from amide groups on the upper rim and the interaction between alkyl chains on the lower rim was proposed.²⁰ Nevertheless, limited tubular structures from calixarenes have been reported so far, and the key structural factors of the building blocks leading to nanotubes, especially sphere-to-tube transitions, have not yet been addressed.

In the family of calixarenes, calix[*n*]crowns, combining the calixarene framework and one or two crown ether loops, have great advantages in self-assembly. The ether loops restrict the original flexible framework, which gives the molecule more regular and controllable self-assembled structures without chemical modification of the bulky head groups. However, investigation on the self-assembly behavior of calix[*n*]crowns, still lacks sufficient attention. Recently, our group demonstrated the morphological transition from vesicles to nanotubes in the self-assembly of calixcrowns.²¹ We found that calix[6]crown molecules bearing two ether loops and two alkyl chain tails (**CamA3**, Scheme 1) gave uniform vesicles in a mixture of water

The Key Laboratory of Molecular Engineering of Polymers, Ministry of Education and Department of Macromolecular Science, Fudan University, Shanghai, 200433, China. E-mail: guanbing_chem@fudan.edu.cn; mjiang@fudan.edu.cn; Fax: (+86) 21-6564-0293

† Electronic supplementary information (ESI) available: Synthesis and characterization details of calix[6]biscrowns, more self-assembly characterizations. CCDC reference number 815175. For ESI and crystallographic data in CIF or other electronic format see DOI: 10.1039/c1jm10895f



Scheme 1 Chemical structures of amphiphilic calix[6]crowns, e.g. **CamA3**, **CamA6**, **Cam2**, **CA5**, **Cca5**. (“C”: calixarenes; “am”: amide; “A”: terminal amine; “ca”: carboxyl group; “n”: number of carbons in the R chain).

and ethanol ($v : v = 1 : 3$). Then, the vesicles were fused into nanotubes by the polarity change of the medium. During this transition, the fusion of vesicles into nanotubes was observed when the water content of the medium was increased. We already proved the importance of the two ether loops for this transition, since its counterpart, which has the same framework but without the loops, turned from vesicles to irregular aggregates with increasing polarity of the medium. However, little was explored regarding the contributions of some structural factors, such as the nature of the terminal groups, the number of carbons in the hydrophobic tails, and the amide linkage between the tails and the backbone, to the self-assembly. On the other hand, the self-assembly into a tubular structure inspired more and more research interest^{22–24} as numerous biologically-generated microtubules with intrinsic functions have been discovered. Thus this article focuses on the key structural factors affecting this morphology transition.

The self-assembly of amphiphilic calix[6]biscrowns shown in Scheme 1 was studied with emphasis on the morphological transition of the assemblies with changing polarity of the medium, and their self-assembly behavior while tuning the medium polarity was investigated. Besides the amino-terminal calix[6]biscrown we reported previously, which has two three-carbon alkyl chains (**CamA3**, Scheme 1), **CamA6**, which has two longer alkyl tails, and **CA5**, which has almost the same tail as **CamA6** but without the amide linkage, were also synthesized. Subsequently, in order to investigate the influence of the end groups, a carboxylic group was introduced to replace the amine end to make **Cca5**. These amphiphilic calix[6]biscrowns were obtained by multi-step synthesis as described in the Experimental section. The obtained molecules were characterized by ¹H NMR spectroscopy and MALDI-TOF mass spectroscopy (Scheme S1, S2, S3 and S4, ESI[†]). The self-assembly behavior of the calix[6]biscrowns in water/ethanol were investigated by a combination of dynamic light scattering (DLS), transmission electron microscopy (TEM), scanning electron microscopy (SEM), atomic force microscopy (AFM) and Fourier transform infrared spectrometry (FT-IR). Additionally, the self-assembly behavior at the air–water interface was also investigated.

2. Results and discussion

The self-assembly behavior of **CamA6** was first investigated, which has six-carbon alkyl chains instead of the three-carbon chains as in the previously studied **CamA3**.^{21a} When deionized water was injected into the ethanol solution of **CamA6**

(1 mg mL⁻¹) as a poor solvent, blue opalescence in the solution was quickly observed, indicating the formation of self-assemblies. Spheres were visualized directly by TEM and SEM (Fig. 1a and 1b) with the diameter ranging from 120 nm to 180 nm as the volume ratio of water/ethanol reached 1 : 1, which was consistent with the data from AFM (Fig. 1c) and DLS (Fig. S1, ESI[†]). It is noteworthy that, when the ratio of water/ethanol reached 3 : 1, spherical structures could not be observed any more, and only tubular aggregates were obtained. The diameter of the nanotubes was found to be around 55 nm and the length reached a micrometre scale (Fig. 1d and 1e). This transition was very similar to the self-assembly behavior of **CamA3**, although higher solvent polarity was required for the transition and broader size distribution was observed. This phenomenon could be attributed to the introduction of the longer alkyl chain, which provides more flexibility to the molecule and may induce looser aggregates.

Moreover, since both **CamA3** and **CamA6** have amide linkages as well as amine ends, we were curious about which would be crucial to obtain the tubular structure when the polarity of the medium was increased. Thus, **CA5**, which has a similar structure to **CamA6** but without the amide linkage (Scheme 1), was designed for this purpose. Through the same approach, vesicles with an average diameter of 140 nm and membrane thickness of 15 nm were observed from the solution of **CA5** (water/ethanol = 1 : 1, Fig. 2a and 2c, SEM results in Fig. S2, ESI[†]). As the polarity of the medium was increased, i.e. water/ethanol 3 : 1, in contrast to **CamA6**, vesicles of **CA5** only tended to dissociate with a little fusion (Fig. 2b). As shown in Fig. S3, ESI[†], the diameter of the obtained structure was smaller than that from the solution with lower polarity (water/ethanol = 1 : 1). The same trend was also monitored by DLS in solution (Fig. 2d). Since particles with a very large size were not detected in the solution of water/ethanol 3 : 1, the observed fusion in TEM probably took place during the process of solvent evaporation in the sample preparation. From analysis of the AFM results, the diameter of the aggregates found in the high polarity medium was about 92 nm and thickness was 9 nm. Upon further increase of the water/ethanol ratio (as high as 10 : 1), no regular tubular

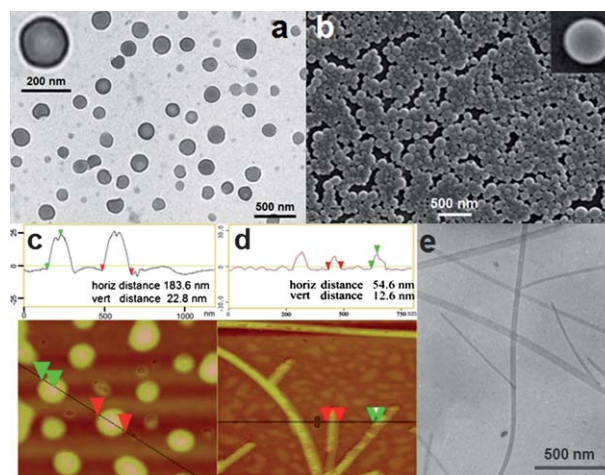


Fig. 1 TEM (a), SEM (b) and AFM (c) images of **CamA6** in water/ethanol ($v : v = 1 : 1$); AFM (d) and TEM (e) images of the tubular aggregates of **CamA6** in water/ethanol ($v : v = 3 : 1$).

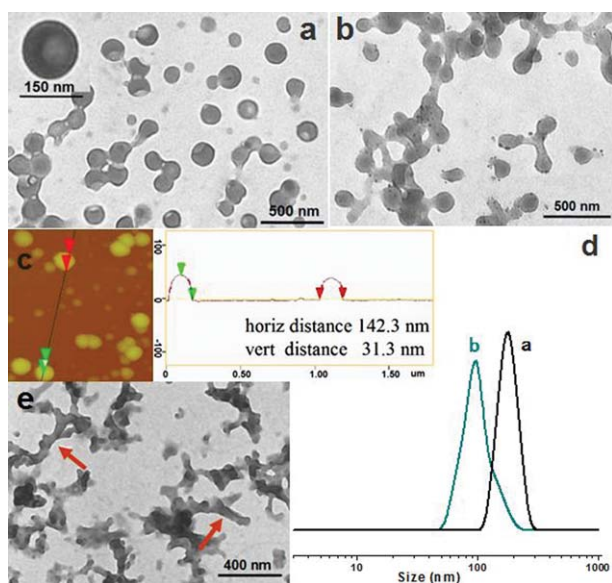


Fig. 2 Images of the aggregates formed by **CA5** in water/ethanol 1 : 1 (TEM (a), AFM (c)) and 3 : 1 (TEM (b)). (d) DLS data of **CA5** in water/ethanol 1 : 1 (line a) and 3 : 1 (line b). (e) TEM image of **CA5** in water/ethanol 10 : 1.

structure was observed, although more fusion of the irregular aggregates appeared, marked by arrows in Fig. 2e.

Comparing the self-assembly behavior of **CamA3** and **CamA6** with **CA5**, the amide linkage seemed an important factor for the transition from vesicles to nanotubes. It is well known that the amide group would form hydrogen bonds, which can be probed by FT-IR.²⁵ For the assembled nanotubes of **CamA6**, compared to the native sample of **CamA6** (in pure ethanol), the wavenumber of N–H and carbonyl stretches shifted from 3395.3 and 1679.4 cm^{-1} to 3352.1 and 1652.4 cm^{-1} respectively (Fig. S4, ESI[†]). The results indicated that hydrogen bonds between the amide groups in the nanotubes are obviously stronger than those in the native state.

Further evidence of this hydrogen bonding came from X-ray single crystal diffractometry. As it was hard to obtain the crystallography data of **CamA6**, instead, we studied compound **Cam2** (Scheme 1). It has the same backbone and the same amide

linkage as in **CamA6**, but with shorter alkyl tails and without the terminal amine, **Cam2** was easier to crystallize. We expected that the result from **Cam2** would help to decipher **CamA6**, because **Cam2** itself can also self-assemble into tubular structures in the same medium of water/ethanol ($v:v = 3 : 1$) as shown in Fig. S5, ESI[†]. The X-ray diffractometry of **Cam2** showed that the distance from N1 to O4 was 2.89 Å (the distance from H1 to O4 is 2.06 Å, Fig. 3 and Fig. S6, ESI[†]), which indicated the existence of an intermolecular hydrogen bond between the two adjacent amide linkages. For each **Cam2**, the –N–H bond on the right amide linkage serves as the proton donor (N–H \cdots O=C) to the carbonyl from its right neighbor calixarene, while the carbonyl group on the left amide acts as the acceptor (C=O \cdots H–N) to the N–H from the neighbor on the other side.

In this study, besides the crown ether loop bridge and the amide linkages, another important factor, the end group of the alkyl tails of the amphiphilic calixcrowns, is discussed. As described in the previous literature, changes in the volume ratio of hydrophilic to hydrophobic parts influenced the molecular curvature, and thus the self-assembled morphology.¹⁷ In our work, instead of an amino group, a carboxylic acid, which has a larger hydrophilic surface than the former, was introduced (**Cca5**). As shown in Fig. 4a and 4c, the TEM and SEM images of **Cca5** indicated the formation of spherical structures in solutions of low water content. With the aid of AFM, the diameter of the spheres was determined to be 80 nm (Fig. 4b), which was consistent with the DLS result (Fig. S7, ESI[†]). The low value of the height of the spherical aggregates (~ 10 nm) indicated the vesicular structure. It is noteworthy that, although having the same rigid molecular framework, the vesicular diameter of **Cca5** aggregates is smaller than that of **CA5**. This result showed that the greater hydrophilic volume of the end group gave a higher molecular curvature, resulting in vesicles with smaller sizes. When the water content of the medium was increased, tubular structures cannot be observed (Fig. S8, ESI[†]), which supports the interpretation of the amide linkage playing an important role in the formation of the nanotubes.

We studied the monolayer behavior of these amphiphilic calixarenes at the air/water interface, which was expected to provide further insight into the difference in their self-assembly in solution.²⁶ Fig. 5 showed the compression isotherms of **CamA6**, **CA5** and **Cca5**. **CamA6** with amide groups gave out a very different

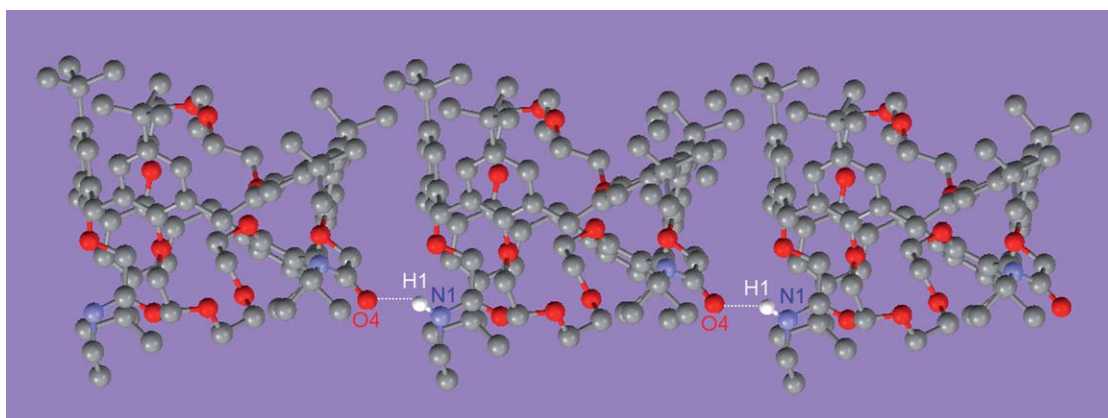


Fig. 3 The X-ray structure of **Cam2**; the distance of the N1 \cdots O4 is 2.89 Å.

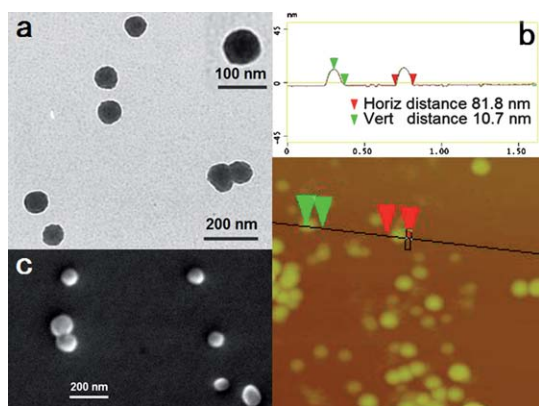


Fig. 4 The TEM (a), AFM (b) and SEM (c) images of **Cca5** in water/ethanol ($v:v = 1 : 2$).

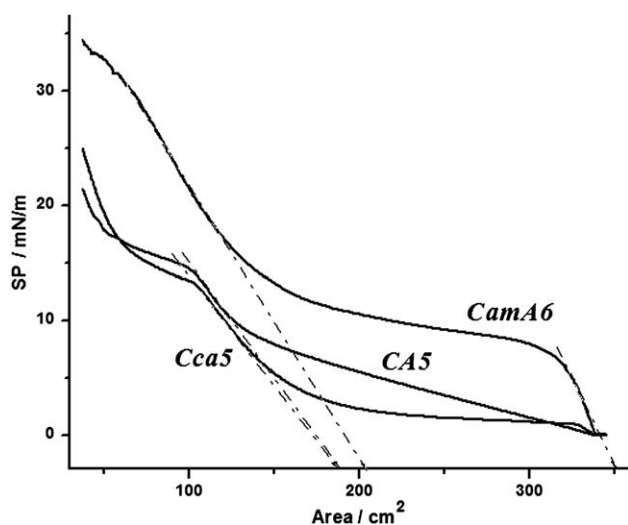


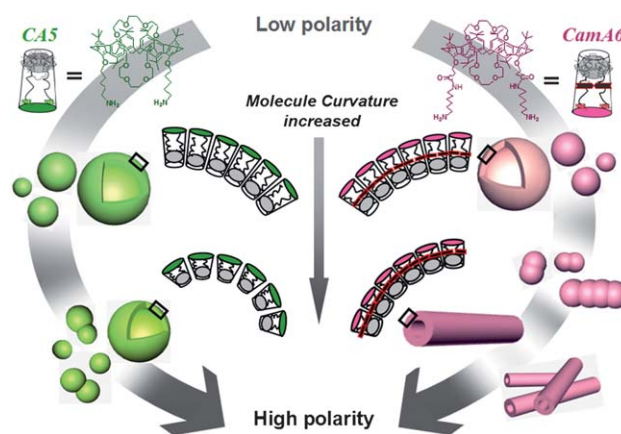
Fig. 5 Surface pressure (π)–area (cm^2) isotherms of **CamA6**, **CA5** and **Cca5**, the dotted lines indicate the limiting area per molecule (A_0).

isotherm from the other two. At the very beginning of the compression (the area of 300–340 cm^2), **CamA6** shows a very sharp surface pressure increase. We presumed that, because of the strong interaction between the amide linkage and water, the amide residues were fully extended on the water/air interface, so **CamA6** had a large extended surface per molecule (352.1 \AA^2). At the surface pressure of about 8 mN m^{-1} , an isothermic platform started. During this compression process, **CamA6** was forced to adjust its orientation from parallel to perpendicular to the air/water interface until the second significant increase of the surface pressure. **CamA6** gave a limiting area (A_0) of 208.2 $\text{\AA}^2/\text{molecule}$, moderately larger than that of **CA5** and **Cca5** (183.5 $\text{\AA}^2/\text{molecule}$ and 182.9 $\text{\AA}^2/\text{molecule}$, respectively). The three numbers are close to the previous reported A_0 for calix[6]arene²⁷ and calix[8]arene,²⁸ where the perpendicular orientation of the molecule was as proposed in the literature. In addition, **CamA6** presented a higher collapse pressure (34.5 mN m^{-1}) than that of **CA5** and **Cca5** (24.97 and 21.52 mN m^{-1}). All of these results gave a clear indication of the distinctive self-assembly behavior of **CamA6** on

a water/air surface under pressure compared to **CA5** and **Cca5**, as a result of the intermolecular interactions of **CamA6** being stronger than those of the other two molecules.

As we just mentioned, calix[n]crowns are a kind of unique building block compared with other types of calixarenes, since the ether loops reduce the flexibility of the framework. However, as the ether loop itself is flexible, its ability to restrain the molecular conformational exchange is limited, so conformational adjustment is still possible. Based on the results mentioned above, we supposed that the strong hydrogen bonding between the amide groups on **CamA6** may provide additional steric hindrance to the conformation change when the medium polarity changed.

Scheme 2 shows our suggestions for the self-assembly mechanism. For the case of the amphiphilic calixcrowns without the amide linkage (**CA5** and **Cca5**), as the polarity of the medium increases, their relatively flexible frameworks allow them to adjust the *tert*-butyl groups and the alkyl chains into a more tightly packed model to decrease the hydrophobic portion, resulting in a higher molecular curvature. The observed change in size of the vesicles of **CA5** and **Cca5** was very large when the medium changed from water/ethanol 1/1 to 3/1, which may involve the dissociation of the large vesicles and re-assembly into small vesicles. Without the strong intermolecular hydrogen bonding the conformational adjustment of **CA5** and **Cca5** is relatively easy and thus makes such reorganization possible. On the other hand, for the case of amphiphilic calixcrowns with amide linkages (**CamA3**, **CamA6** and **Cam2**), in the initial vesicles in water/ethanol 1/1, the molecules are linked by strong intermolecular hydrogen bonding. Thus, when the medium polarity increases, the conformational adjustment of the individual molecules is, to some extent, restricted and thus the dissociation and re-assembly would be very difficult. Therefore, in response to the increase in medium polarity, the initial vesicles tend to link to each other and extend on the axis direction accompanying a compression on the plane perpendicular to the axis, and then gradually fuse into nanotubes. Obviously, in this process, much less conformational adjustment is required than for the large vesicles transforming into small ones.



Scheme 2 Schematic representation for morphology transitions in self-assembly of **CamA6** and **CA5** with changes in medium polarity.

3. Experimental section

General procedures

All materials and reagents were used directly from commercial suppliers unless mentioned. **CamA6**, **CA5** and **Cca5** were synthesized from a calix[6]biscrown precursor²⁹ separately as shown in Scheme S1–S3, ESI.† In order to obtain the self-assembled aggregates, distilled water was injected into the ethanol solutions of the calix[6]biscrowns to give different volume ratios of water/ethanol. Transmission Electron Microscopy (TEM) was performed on a Philips CM 120 electron microscope. A small droplet of the solution was deposited onto a carbon-coated copper grid, and then dried at room temperature. Scanning Electron Microscopy (SEM) experiments were performed on a Tescan 5136MM scanning electron microscope. Atomic Force Microscopy (AFM) images were acquired in tapping mode using a Nanoscope IV from Digital Instruments equipped with a silicon cantilever with a 125 Pmand E-type vertical engage piezoelectric scanner. For SEM and AFM observations, the samples were prepared on freshly cleaved mica and dried at room temperature. Dynamic Light Scattering (DLS) results were obtained on an Autosizer 4700 after filtration through a PTFE membrane. Fourier Transform Infrared (FT-IR) spectra were obtained on a Magna-550 FT-IR instrument (quick evaporation of sample solution on CaF₂ tablet). ¹H-NMR was carried out on a Bruker (500 MHz) NMR instrument, using tetramethylsilane (TMS) as reference and CDCl₃ as solvent. Matrix-Assisted Laser Desorption Ionization Time-of-Flight Mass Spectroscopy (MALDI-TOF MS) analysis was performed on a Voyager-DE STR with the accelerating potential of 20 kV. The surface pressure–area (π -A) isotherm was measured in the High Performance Alternate Layer Combination System (KSV 2000) with the water subfaces (pH 6.80 and 25 °C). After evaporation of the organic solvent (chloroform), the monolayer was compressed using two symmetric barriers with a compression velocity of 15.0 mm min⁻¹. The measurements were repeated several times and the isotherms were reproducible. X-ray single crystal data are shown in detail in Table S1, ESI.†

4. Conclusion

We synthesized and characterized amphiphilic calix[6]biscrown derivatives with different structural characteristics. In the study of their self-assembly in solution, we found that **CamA6**, with an amide linkage between the backbone and alkyl tails, gave a clear transition from vesicles to nanotubes when the content of water in solution was increased. For **CA5** and **Cca5**, without such an amide linkage, only size decreases of the vesicular structures upon the same change in medium were displayed. Furthermore, the FT-IR analysis of **CamA6** and the crystallographic data of its analog **Cam2**, as well as the difference in the air/water interface behavior of **CamA6** compared with **CA5** and **Cca5**, pronounced the key effect of the amide residue in forming intermolecular hydrogen bonds in the self-assembly.

These results provide a clear view of the relationship between specific molecular structures and aggregation morphologies of the calix[6]biscrowns: Firstly, not only the bridging crown ether loops, but also the amide linkage between the backbone and the tails, contributed to the structural transition from vesicles to

nanotubes; Secondly, the replacement of the terminal groups of the tails can efficiently adjust the size of spherical aggregates. Such results will be promising to manipulate novel and exciting functional materials with controllable size and morphology based on calixcrowns.

Acknowledgements

National Natural Science Foundation China (No. 20774021 and No. 20834004) and Ministry of Science and Technology of China (2009CB930402 and 2011CB932503) are acknowledged for financial support. We also thank Jie Sun from State Key Laboratory of Organometallic Chemistry, SIOC, CAS and Prof. Linhong Weng from Department of Chemistry, Fudan University for their generous help to determine the X-ray Single Crystal Diffractometry data.

References

- (a) G. M. Whitesides and B. Grzybowski, *Science*, 2002, **295**, 2418–2421; (b) S. Forster and T. Plantenberg, *Angew. Chem., Int. Ed.*, 2002, **41**, 688–714.
- J. B. F. N. Engberts and J. Kevelam, *Curr. Opin. Colloid Interface Sci.*, 1996, **1**, 779–789.
- (a) M. Kogiso, Y. Zhou and T. Shimizu, *Adv. Mater.*, 2007, **19**, 242–246; (b) C. Park, M. S. Im and C. Kim, et al, *Angew. Chem., Int. Ed.*, 2008, **47**, 9922–9926.
- E. T. Pashuck and S. I. Stupp, *J. Am. Chem. Soc.*, 2010, **132**, 8819.
- Y.-b. Lim, K. S. Moon and M. Lee, *Chem. Soc. Rev.*, 2009, **38**, 925–934.
- M. A. C. Stuart, W. T. S. Huck, I. Luzinov and S. Minko, et al., *Nat. Mater.*, 2010, **9**, 101–113.
- B. Trappmann, K. Ludwig, M. Ç. R. Radowski, A. Shukla, A. Mohr, H. Rehage, C. BoÄattcher and R. Haag, *J. Am. Chem. Soc.*, 2010, **132**, 11119–11124.
- (a) X. H. Yan, Q. He, K. W. Wang, L. Duan, Y. Cui and J. B. Li, *Angew. Chem., Int. Ed.*, 2007, **46**, 2431–2434; (b) X. H. Yan, Y. Cui, Q. He, K. W. Wang, J. B. Li, W. H. Mu, B. L. Wang and Z. C. Ou-yang, *Chem.–Eur. J.*, 2008, **14**, 5974–5980.
- (a) G. W. Orr, L. J. Barbour and J. L. Atwood, *Science*, 1999, **285**, 1049–1052; (b) R. Zadnand and T. Schrader, *J. Am. Chem. Soc.*, 2005, **127**, 904–915; (c) A. Ikeda and S. Shinkai, *Chem. Rev.*, 1997, **97**, 1713–1734; (d) Y. Rudzевич, V. Rudzевич, C. Moon, I. Schnell, K. Fischer and V. Bohmer, *J. Am. Chem. Soc.*, 2005, **127**, 14168–14169.
- (a) K. S. Kim, S. B. Suh and J. C. Kim, et al., *J. Am. Chem. Soc.*, 2002, **124**, 14268–14279; (b) V. Sidorov, F. W. Kotch, M. El-Kouedi and J. T. Davis, *Chem. Commun.*, 2000, 2369–2370.
- S. Saito, D. M. Rudkevich and J. Rebek, *Org. Lett.*, 1999, **1**, 1241–1244.
- D. M. Homden and C. Redshaw, *Chem. Rev.*, 2008, **108**, 5086–5130.
- (a) O. M. Martin and S. Mecozzi, *Tetrahedron*, 2007, **63**, 5539–5547; (b) O. M. Martin, L. Yu and S. Mecozzi, *Chem. Commun.*, 2005, 4964–4966.
- S. Houmadi, D. Coquiere, L. Legrand, M. C. Faure, M. Goldmann, O. Reinaud and S. Remita, *Langmuir*, 2007, **23**, 4849–4855.
- (a) S. Jebors, B. Lesniewska, O. Shkurenko, K. Suwinska and A. W. Coleman, *J. Inclusion Phenom. Macrocyclic Chem.*, 2010, **68**, 207–217; (b) S. Jebors, G. S. Ananchenko, A. W. Coleman and J. A. Ripmeester, *Tetrahedron Lett.*, 2007, **48**, 5503–5506.
- (a) X. Yu, C. L. Tu, L. He, R. B. Wang, G. M. Sun, D. Y. Yan and X. Y. Zhu, *J. Macromol. Sci., Part A: Pure Appl. Chem.*, 2009, **46**, 360–367; (b) K. Wang, D. S. Guo and Y. Liu, *Chem.–Eur. J.*, 2010, **16**, 8006–8011.
- M. Lee, S. J. Lee and L. H. Jiang, *J. Am. Chem. Soc.*, 2004, **126**, 12724–12725.
- M. Kellermann, W. Bauer, A. Hirsch, B. Schade, K. Ludwig and C. Bottecher, *Angew. Chem., Int. Ed.*, 2004, **43**, 2959–2962.
- M. Strobel, K. Kita-Tokarczyk, A. Taubert, C. Vebert, P. A. Heiney, M. Chami and W. Meier, *Adv. Funct. Mater.*, 2006, **16**, 252–259.

- 20 Y. Sun, C. G. Yan, Y. Yao, Y. Han and M. Shen, *Adv. Funct. Mater.*, 2008, **18**, 3981–3990.
- 21 (a) B. Guan, M. Jiang, X. Yang, Q. Liang and Y. Chen, *Soft Matter*, 2008, **4**, 1393–1395; (b) B. Guan, Q. Liang, Y. Zhu, M. Qiao, J. Zou and M. Jiang, *J. Mater. Chem.*, 2009, **19**, 7610–7613; (c) Q. Liang, B. Guan and M. Jiang, *J. Mater. Chem.*, 2010, **20**, 8236–8239; (d) Q. Liang, B. Guan and M. Jiang, *Progress in Chemistry*, 2010, **22**, 388–399.
- 22 T. Shimizu, M. Masuda and H. Minamikawa, *Chem. Rev.*, 2005, **105**, 1401–1444.
- 23 U. Raviv, D. J. Needleman, Y. L. Li, H. P. Miller, L. Wilson and C. R. Safinya, *Proc. Natl. Acad. Sci. U. S. A.*, 2005, **102**, 11167–11172.
- 24 J. M. Zayed, N. Nouvel, U. Rauwald and O. A. Scherman, *Chem. Soc. Rev.*, 2010, **39**, 2806–2816.
- 25 N. Yamada, K. Ariga, M. Naito, K. Matsubara and E. Koyama, *J. Am. Chem. Soc.*, 1998, **120**, 12192–12199.
- 26 G. de Miguel, J. M. Pedrosa, M. T. Martin-Romero, E. Munoz, T. H. Richardson and L. Camacho, *J. Phys. Chem. B*, 2005, **109**, 3998–4006.
- 27 L. Dei, A. Casnati, P. L. Nostro and P. Baglioni, *Langmuir*, 1995, **11**, 1268–1272.
- 28 F. Davis, L. O'Toole, R. Short and C. J. M. Stirling, *Langmuir*, 1996, **12**, 1892–1894.
- 29 B. Guan, S. L. Gong, X. J. Wu, Z. G. Li and Y. Y. Chen, *J. Inclusion Phenom. Macrocyclic Chem.*, 2006, **54**, 81–84.